



Meso-scale modelling of shock wave propagation in a SiC/Al nanocomposite reinforced with WS₂-inorganic fullerene nanoparticles

E.I. Volkova^{a,b}, I.A. Jones^{a,*}, R. Brooks^a, Y. Zhu^c, E. Bichoutskaia^b

^a Division of Materials, Mechanics and Structures, Faculty of Engineering, University of Nottingham, Nottingham NG7 2RD, United Kingdom

^b School of Chemistry, University of Nottingham, Nottingham NG7 2RD, United Kingdom

^c College of Engineering, University of Exeter, Exeter EX4 4QF, United Kingdom

ARTICLE INFO

Article history:

Available online 13 September 2012

Keywords:

Nanocomposite structures
Meso-scale modelling
Shock wave propagation
Finite element analysis

ABSTRACT

It has been postulated that nanocomposites incorporating IF-WS₂ nanoparticles within a strong matrix might form the next generation of highly shock-resistant materials. The present work describes initial analyses into the shock response of such materials via a sequential multi-scale dynamic analysis. Density functional theory is used to calculate the elastic properties of the multilayered WS₂ nanoparticles. These properties are then used within an explicit finite element (FE) analysis of wave propagation through an embedded statistical volume element (SVE) of a two-phase nanocomposite consisting of a matrix with IF-WS₂ nanoparticles. Some wave front dispersion was noted, particularly where the modulus of the matrix is significantly different from that of the particles. A three-phase nanocomposite consisting of an aluminium matrix with IF-WS₂ and SiC nanoparticles was also considered, and showed more apparent wave front dispersion than for the two-phase nanocomposite. Hugoniot shock propagation data have been derived from the simulation outputs. It is concluded that sequential multiscale modelling of these systems is appropriate and can provide useful information about shock wave propagation in the elastic region. The work also provides a foundation for more realistic simulations at higher rate loading, where it will be necessary to incorporate material failure in the models.

© 2012 Elsevier Ltd. All rights reserved.

1. Introduction

It has been found that ceramic/metal nanocomposites reinforced with nanomaterials have the potential to withstand static loading conditions as well as conditions under high rate loads [1]. Nanomaterials such as inorganic fullerene-like (IF) nanomaterials have already been shown to have high strength and hardness [2–4]. Consequently, it can be postulated that nanocomposites, reinforced with IF-WS₂ nanoparticles, have a potential to improve shock-absorbing properties. Understanding the shock propagation and attenuation properties of these systems, and how the behaviour is controlled by the nano-structure and constituents, is paramount if optimum systems are to be designed under these conditions. The aim of this work is therefore to develop a meso-scale modelling approach that accurately represents and simulates the real nanocomposite structure, morphology and behaviour of a nanocomposite reinforced with IF-WS₂ nanoparticles under dynamic loading. The simulations have been performed with the ABAQUS explicit finite element code. The material properties of IF-WS₂ layered bulk material were previously computed using

density functional theory at the atomistic level [5] and are used here to represent the components of the nanoparticle stiffness matrix in the finite element model. The influence of volume fraction, constituent properties and loading conditions in the finite element unit cell on the mechanical response and shock wave propagation through the material are investigated.

2. Finite element model

The models of shock wave propagation in an IF-WS₂-containing nanocomposite have been performed using a statistical volume element (SVE) implemented within the ABAQUS/Explicit finite element system. The SVE, as shown in Fig. 1, has randomly distributed particles in a matrix, with the structure having no particular directionality. The IF-WS₂ takes the form of multilayered nanoparticles, in some cases approaching a spherical shape with almost no defects in curvature [6]. For the present purposes these are idealised as being hollow and perfectly spherical, with the multilayered walls of the nanoparticle being represented as a transversely isotropic material, having the elastic properties of layered, bulk WS₂, with its local directions defined with reference to a spherical coordinate system.

* Corresponding author. Tel.: +44 (0) 115 9513784.

E-mail address: arthur.jones@nottingham.ac.uk (I.A. Jones).

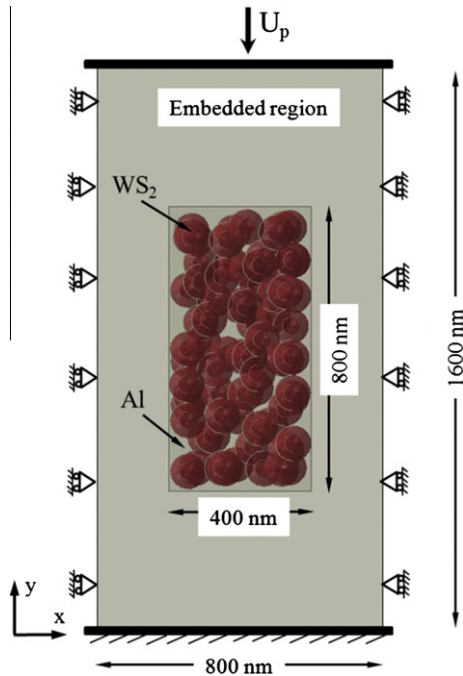


Fig. 1. The SVE boundary conditions.

No reliable mechanical properties could be found for layered WS_2 , so these were predicted ab initio using density functional theory [5]. The bulk structure of layered WS_2 bulk was modelled using a unit cell of six atoms implemented within the CASTEP 5.5 quantum chemistry program [7]. In order to validate this approach, the structural parameters (lattice spacings) and elastic properties of

MoS_2 were predicted using DFT and were compared against the body of existing experimental and computational results, with which they were found to be mostly in very good agreement. This gave confidence in applying the prediction method to WS_2 . The structural parameters predicted for WS_2 were indeed very close to published values. The elastic properties (in the form of the elastic stiffness matrix, or equivalently in the form of engineering constants consisting of Young's moduli, shear moduli and Poisson's ratios) were as expected found to be those of a transversely isotropic material and were taken forward for use in subsequent analyses. The ab initio prediction of the properties of MoS_2 and WS_2 , and an initial example of their use within a static (implicit) FE model of a nanocomposite, are described in detail in Volkova et al. [5], with the combination of the DFT and FE models forming a sequential multi-scale modelling approach. Computed mechanical properties and particle dimensions used as input to the ABAQUS SVE are given in Table 1. Material properties of the embedded region have been obtained using the theory of Budiansky [8]. In this theory, the elastic properties of the embedded region are obtained as aggregate elastic constants of an inhomogeneous material using Eshelby's inclusion technique [9].

The embedded and rolling boundary conditions are implemented as shown in Figs. 1 and 8. A particle velocity, U_p was applied to the top face of the SVE in the case of two phase nanocomposite (or to a top of the embedded boundary in case of three phase nanocomposite) as a prescribed velocity boundary condition. At the beginning of simulations the amplitude of U_p is ramped up according to the quadratic function of time to avoid influence of the top boundary [11]. The bottom face of the SVE (or the embedded region) is fixed against any movements. 'Rolling' boundary conditions, which do not allow any displacements in the normal direction, are applied to the remaining faces of the SVE (or embedded region). In order to avoid secondary shockwave propagations, the simulations have been terminated when the shock

Table 1
Mechanical properties of materials for the FEM analysis.

	Young's modulus, E (GPa)	Poisson's ratio, ν	Radius (nm)	Density, ρ (g/cm ³)	
Al [10]	70	0.35	Matrix	2.7	
SiC [10]	400	0.19	400 or matrix	3.21	
WS_2 [5]	Longitudinal (circumferential)	224	ν_{21}	50	7.5
	Transverse (radial)	42	ν_{13}		
			ν_{23}		

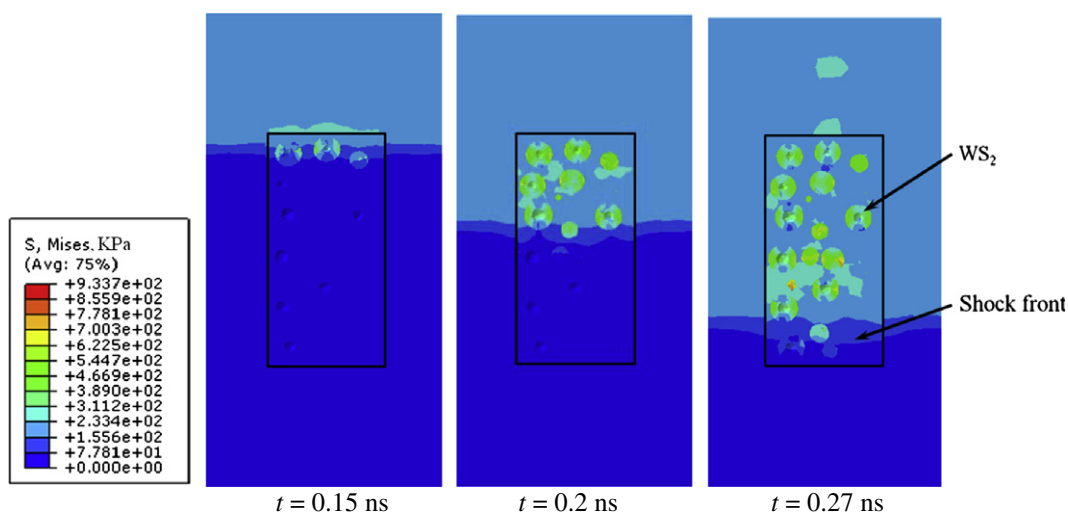


Fig. 2. Contours of the stress wave propagation in Al/ WS_2 nanocomposite with 25.4% WS_2 .

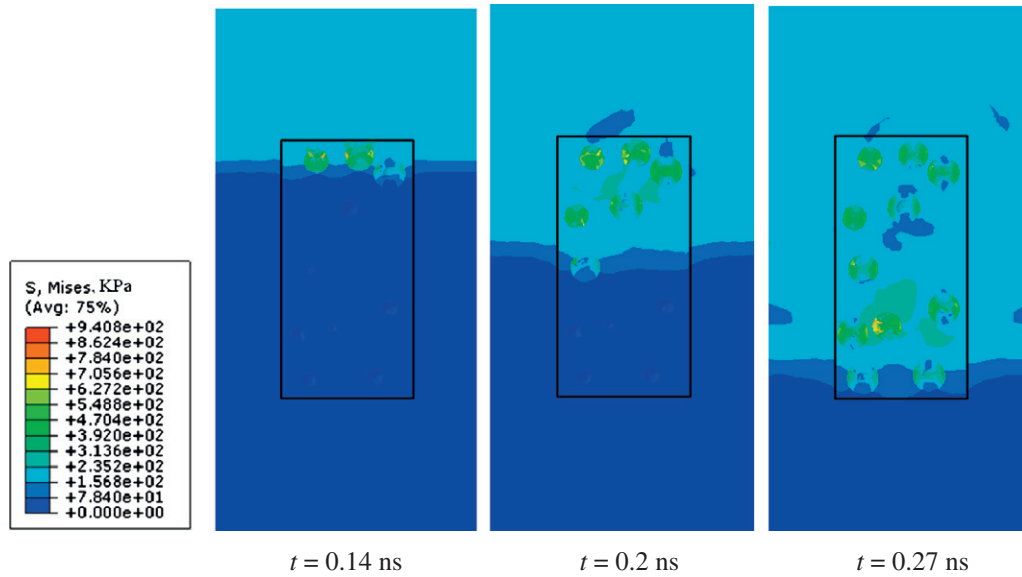


Fig. 3. Contours of the stress wave propagation in Al/WS₂ nanocomposite with 13.2% WS₂.

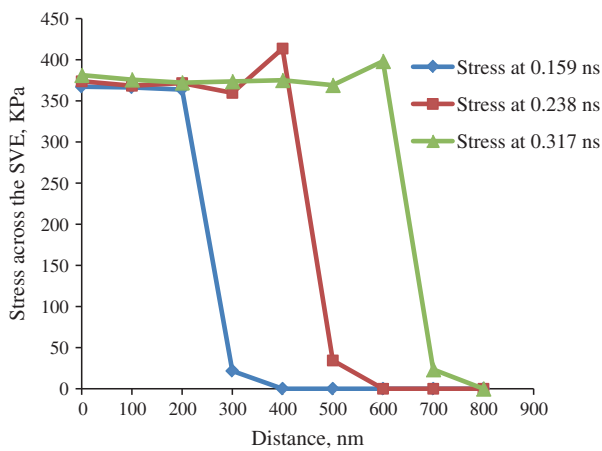


Fig. 4. Averaged compression stress across the SVE for Al matrix with 25.4% IF-WS₂ at time steps of 0.159 ns, 0.238 ns and 0.317 ns.

wave front has reached 90–95% of the SVE (embedded region) depth [11].

3. Results and discussion

3.1. Two phase nanocomposite

3.1.1. Shock wave propagation and dispersion

The wave propagation in the two phase nanocomposite (25.4% WS₂ in Al matrix) SVE model, with embedded boundary conditions, is shown in Fig. 2. The stress in the y direction is shown at different time intervals. The shock wave shows some dispersion and stress variation behind the shock front as stress propagates through the IF-WS₂ faster than through the Al matrix resulting in stress fingering. At reduced volume fraction (13.2% WS₂), as shown in Fig. 3, this stress fingering is lower resulting in a more planar compaction wave. Thus, the volume fraction of nanoparticle inclusions does affect the degree of dispersion.

Fig. 4 shows the average normal compression stress (y-stress) across the SVE at 100 nm intervals down the element at three time

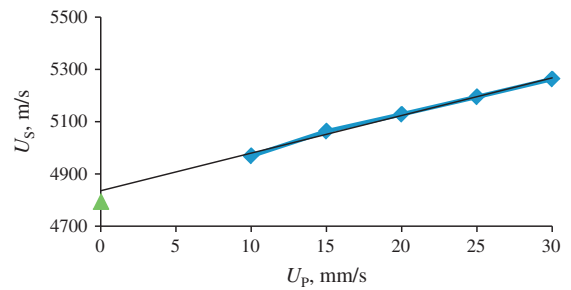


Fig. 5. Hugoniot data obtained from simulations. U_S-U_P relations for the Al/WS₂ nanocomposite (25.4% WS₂). A is the acoustic wave speed through the equivalent aggregate material.

steps for the 25.4% volume fraction case. This clearly shows the progression of the shock front. It commences with a steep edge but progressively slopes as dispersion of the wave front takes place. Fig. 5 is a plot of the shock speed (U_S) vs. particle speed (U_P) Hugoniot, obtained from a range of simulations at different impact (particle) speeds. As reported previously for other material systems [12], there is a linear relationship between U_S and U_P and extrapolation back to zero U_P gives a wave speed approximately corresponding to the acoustic wave speed (C_0) of the system, indicated by the point at 4795 m/s on the axis. The latter has been calculated, corresponding to a material laterally restrained with rolling boundary conditions, from the following equation:

$$C_0 = \sqrt{\frac{C_{11}}{\rho}}$$

where C_{11} is the component of the stiffness matrix of the aggregate material and ρ is the density as calculated for the embedding material. This agreement with the acoustic wave speed is confirmation that the simulations are predicting shock propagation correctly.

3.1.2. Effect of mismatch of material properties: SiC/WS₂ system

It is instructive to explore what the effect of having a greater mismatch between the moduli of the constituents as for the Al/WS₂ system there is the close value for modulus of the aluminium matrix (70 GPa) to the effective isotropic modulus of the WS₂

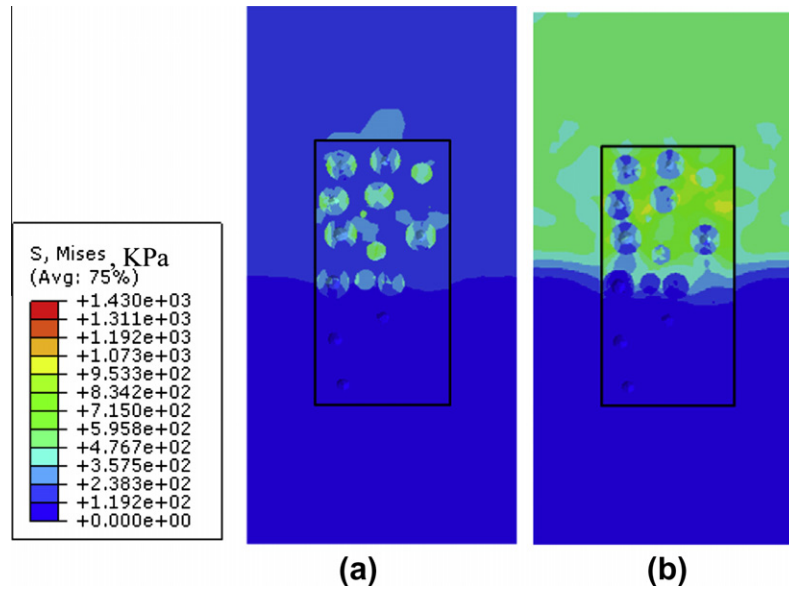


Fig. 6. Normal stress wave propagation in nanocomposites: (a) Al/WS₂ and (b) SiC/WS₂.

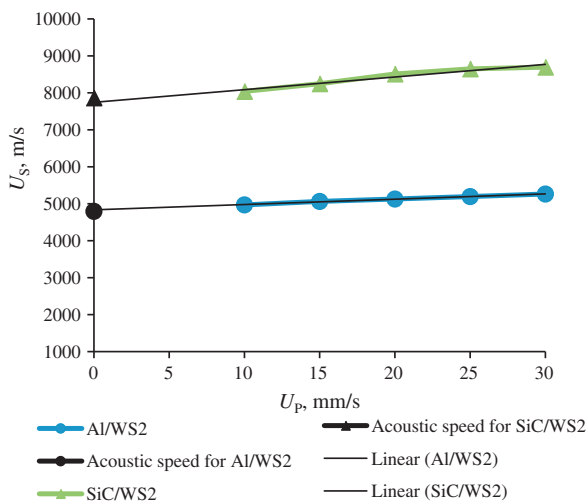


Fig. 7. Hugoniot data obtained from simulations. U_S-U_P relations for Al/WS₂ and SiC/WS₂ nanocomposites and corresponding acoustic wave speeds.

inclusions, computed to be 60 GPa. A sensitivity study has therefore been performed by setting the matrix to Silicon Carbide (SiC), i.e. compared with WS₂ (60 GPa), matrix with a high modulus (400 GPa). Note that this system does not represent real material but is used purely for illustration purposes within the sensitivity study. The result of the simulation, when the shock wave has traversed half of the SVE length, is compared with the Al/WS₂ system in Fig. 6. The SiC/WS₂ system shows significant stress variation indicative of dispersion, with stresses in this case, as expected, very much higher in the stiff SiC matrix than in the inclusions. For this system, the mismatch of moduli is 400 GPa/60 GPa \approx 7. Stress fingering at the shock front is more pronounced than the Al/WS₂ system. In general, it can be concluded that a greater mismatch of moduli between matrix and inclusions results in a greater degree of dispersion as evidenced by stress fingering and/or stress variations.

Fig. 7 shows that both systems exhibit the expected U_S-U_P Hugoniot linear relationships, extrapolating back to the acoustic

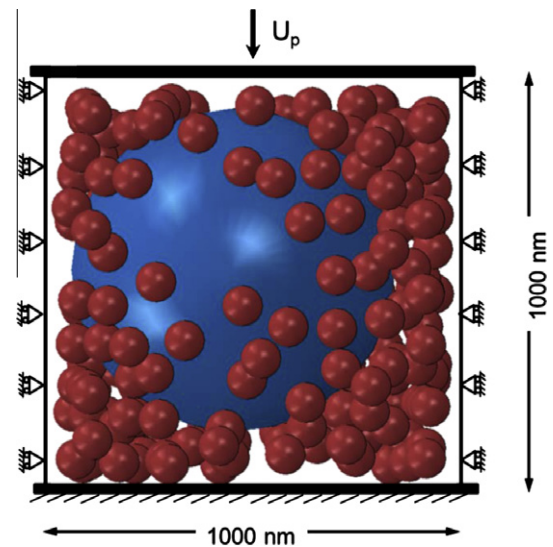


Fig. 8. The SVE model for a 3 phase SiC/Al/WS₂ nanocomposite.

wavespeeds. The SiC/WS₂ system exhibits the highest shock speeds due to its higher effective modulus.

3.2. Three phase nanocomposite

An SVE model for a three-phase system has also been studied. The system comprises SiC/Al composite (26.8% SiC), reinforced with 8.75% IF-WS₂ nano inclusions as shown in Fig. 8. This is representative of a typical armour material (SiC/Al) but reinforced with hard nano inclusions. The micro scale ceramic particle is embedded in the Al matrix and surrounded with a random distribution of the nano scale WS₂ inclusions. To simplify the analysis, rolling boundary conditions are applied directly to the composite region rather than embedding it in an isotropic buffer zone. A particle velocity has also been applied directly to the SVE cell. As in the case of two phase nanocomposite the bottom face of the SVE is fixed. Previous analysis of the two-phase systems has shown that these boundary conditions give similar results to the embedded

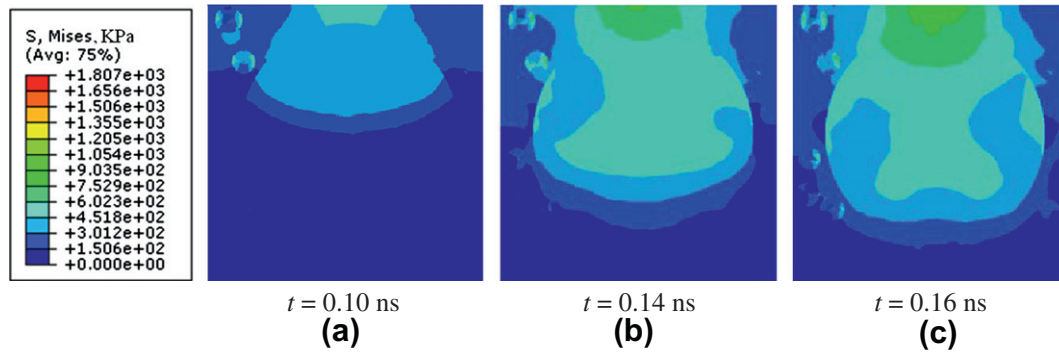


Fig. 9. Stress wave propagation in a SiC/Al/WS₂ nanocomposite.

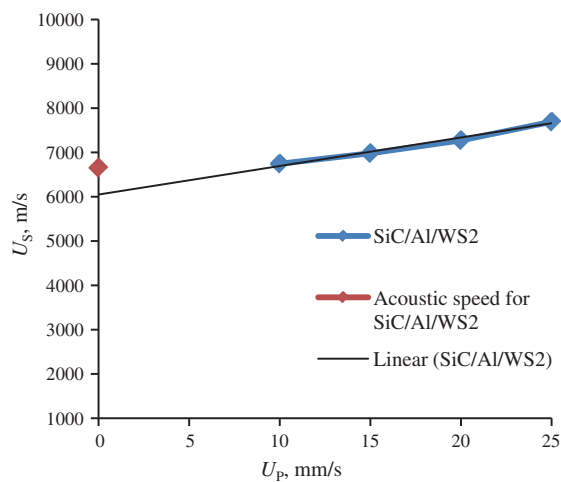


Fig. 10. Hugoniot data obtained from simulations. U_S-U_P relations for the SiC/Al/WS₂ nanocomposite (26.8% SiC and 8.75% WS₂). \diamond is the acoustic wave speed through the equivalent aggregate material.

boundary conditions, in spite of the greater constraint against local lateral displacements.

The wave propagation through the three phase nanocomposite is shown in Fig. 9. The stress in the y direction is shown propagating through the material at three points in time. It is clear that the wave has a high propagation speed through the ceramic particle extending the wave front in this region. This is effectively stress fingering, but on a micro scale rather than a nano scale. In addition, the nano inclusions do have some dispersive effect at the wave front. As for the two-phase systems, Hugoniot data in the form of a U_S vs. U_P plot can also be generated from this model by impacting at different speeds, as shown in Fig. 10.

4. Conclusion

It has been shown that a statistical volume element (SVE) approach in an elastic FE analysis can model the dynamic response of a two and three-phase nanocomposite in some detail. The

simulation of shock wave progression through the SVE has shown evidence of stress fingering and dispersion caused by the nano inclusions and that these effects are influenced by volume fraction of inclusions and mismatch of constituent stiffnesses, i.e. moduli. A greater mismatch results in greater dispersion of the wave front. Shock speed vs. particle speed Hugoniot data has also been generated from the models. Successful simulation of the shock wave propagation and comparisons with the value(s) of the acoustic wave speed provide the confidence that the numerical technique is suitable for more complex and realistic simulations including implementation of failure mechanisms. This will be necessary to fully simulate the material response under very high rates of loading such as that occurring during blast and ballistic conditions.

Acknowledgements

The authors are grateful to the Engineering and Physical Research Council for funding this project under Grant EP/G039879/2 (co-funded by the Ministry of Defence (MoD) under the Joint Academic Research Programme for Defence) and for funding E. Bichoutskaia's position via a EPSRC Career Acceleration Fellowship EP/G005060/1, and to the University of Nottingham for co-funding the studentship of E.I. Volkova. We are also grateful to Professor G. Seifert for fruitful and constructive discussions.

References

- [1] Rapoport L, Lvovsky M, Lapsker I, Leshchinsky V, Volovik Yu, Feldman Y, et al. NanoLett 2001;1:137.
- [2] Zhu YQ, Sekine T, Li YH, Wang WX, Fay MW, Edwards H, et al. Adv Mater 2005;17:1500.
- [3] Zhu YQ, Sekine T, Li YH, Fay MW, Zhao YM, Patrick Poa CH, et al. J Am Chem Soc 2005;126:16253.
- [4] Zhu YQ, Sekine T, Brigatti KS, Firth S, Tenne R, Rosentsveig R, et al. J Am Chem Soc 2003;127:1329.
- [5] Volkova EI, Jones IA, Brooks R, Zhu Y, Bichoutskaia E. Phys Rev B, in press.
- [6] Tenne R, Homyonfer M, Feldman Y. Chem Mater 1998;10:11.
- [7] Clark SJ, Segall MD, Pickard CJ, Hasnip PJ, Probert MIJ, Refson K, et al. Z Kristallogr 2005;220:567.
- [8] Budiansky B. J Mech Phys Solids 1965;13:223.
- [9] Eshelby JD. Proceed Royal Soc A 1957;241:376.
- [10] Callister WD, Rethwisch DG. Material science and engineering: an introduction. Wiley; 2010.
- [11] Austin RA, McDowell DL, Benson DJ. Modelling Simul Mater Sci Eng 2006;14:537.
- [12] Davison L. Fundamentals of shock wave propagation in solids. Springer; 2008.